PHYSICAL REVIEW B, VOLUME 63, 041403(R)

Partial density of occupied valence states by x-ray standing waves and high-resolution photoelectron spectroscopy

J. C. Woicik and E. J. Nelson
Materials Science and Engineering Laboratory, National Institute of Standards and Technology, Gaithersburg, Maryland 20899

T. Kendelewicz and P. Pianetta
Stanford Synchrotron Radiation Laboratory, Stanford University, Stanford, California 94305

Manish Jain, Leeor Kronik, and James R. Chelikowsky
Department of Chemical Engineering and Materials Science, University of Minnesota, Minneapolis, Minnesota 55455
(Received 7 July 2000; revised manuscript received 7 November 2000; published 9 January 2001)

We introduce an experimental method by which site-specific valence-electronic structure may be obtained. It utilizes the spatial dependence of the electric-field intensity that results from the superposition of the incident and reflected x-ray beams within the vicinity of a crystal x-ray Bragg reflection. Resolution of the anion and cation contributions to the GaAs valence band is demonstrated and compared to an *ab initio* theoretical calculation of the Ga and As partial density of states.

DOI: 10.1103/PhysRevB.63.041403 PACS number(s): 79.60.−i

One of the most powerful experimental tools for examining the electronic structure of a solid or film is photoelectron spectroscopy. Due to the conservation of energy between the incident photon and the ejected photoelectron,[1] direct and important electronic information pertaining to the occupied valence-band density of states has been obtained for many materials. This information has been used to establish the validity of complicated band-structure calculations for metals, semiconductors, insulators, and alloys.[2]

Typical photoemission measurements are performed with excitation sources that are assumed to be monochromatic plane waves. As the intensity of a plane wave is constant over the dimensions of the crystalline-unit cell, standard photoemission measurements are unable to produce *direct*, site-specific valence information. However, such information is important for advancing our understanding of how chemical bonding results in the solid-state electronic structure.

This limitation of the photoemission technique has been partially mitigated by experiments that have exploited either the photon-energy dependence or Cooper minimum[3] of the atomic cross sections of the atoms within the unit cell,[4–6] or the Fano[7] resonant behavior of these atoms near a core-ionization threshold.[8] Additionally, x-ray photoelectron diffraction, utilizing the phase and scattering amplitudes of the different atoms within the unit cell, has also been used to obtain site-specific information.[9]

Here we describe an experimental method for obtaining site-specific valence-electronic structure. Unlike the methods described above that rely on the detailed atomic properties of the individual atoms within the unit cell, it utilizes only the spatial variation of the electric-field intensity that occurs within the vicinity of a crystal x-ray Bragg reflection. Under the condition of x-ray Bragg diffraction, the spatial dependence of the electric field is given by the superposition of the incident $\mathbf{E}_o$ and reflected $\mathbf{E}_h$ x-ray beams that travel with wave vectors $\mathbf{k}_o$ and $\mathbf{k}_h$, polarization vectors $\hat{\mathbf{e}}_o$ and $\hat{\mathbf{e}}_h$, and frequency ω:

$$\mathbf{E}(\mathbf{r},t)=[\hat{\mathbf{e}}_o E_o e^{i\mathbf{k}_o\cdot\mathbf{r}}+\hat{\mathbf{e}}_h E_h e^{i\mathbf{k}_h\cdot\mathbf{r}}]e^{-i\omega t}. \quad (1)$$

$\mathbf{k}_o$ and $\mathbf{k}_h$ are connected by the Bragg condition $\mathbf{h}=\mathbf{k}_h-\mathbf{k}_o$, where $\mathbf{h}$ is a reciprocal-lattice vector of the crystal. For the σ-polarization geometry of a symmetric reflection, this field squares to give the electric-field intensity at an arbitrary point $\mathbf{r}$ in space:

$$I(\mathbf{r})=|E_o|^2[1+R+2\sqrt{R}\cos(\nu+\mathbf{h}\cdot\mathbf{r})]. \quad (2)$$

ν is the phase of the complex-field amplitude ratio $E_h/E_o=\sqrt{R}e^{i\nu}$, and R is the reflectivity function $R=|E_h/E_o|^2$. Germane to the method is the unique ability to position the maxima (or minima) of the electric-field intensity at any location within the crystalline-unit cell by experimentally varying the phase of the complex reflectivity function between $0<\nu<\pi$. This is achieved by slightly varying either the sample angle or the photon energy within the natural width of the crystal x-ray Bragg reflection.[10]

Because the probability of emission of an electron from an atom in an external electric field is proportional to the electric-field intensity at the location of its atomic core (dipole approximation[11]), by selectively positioning the electric-field intensity within the unit cell and recording high-resolution valence-photoelectron spectra, spatially resolved components to the photoemission valence-band density of states may be directly obtained.

To illustrate the principle of the technique, Fig. 1 shows a theoretical calculation of the electric-field intensities and their spatial dependence relative to the GaAs atomic planes at the GaAs(111) and GaAs($\bar{1}\bar{1}\bar{1}$) Bragg back-reflection conditions for photon energy $\hbar\omega=1900.05$ eV. The calculation uses the electric-field intensity [Eq. (2)], together with the photon-energy dependence of R and ν as calculated from the dynamical theory of x-ray diffraction.[10] For the (111) reflection $\mathbf{h}=2\pi[111]/a$, and for the ($\bar{1}\bar{1}\bar{1}$) reflection $\mathbf{h}=2\pi[\bar{1}\bar{1}\bar{1}]/a$, where a is the GaAs lattice parameter equal to 5.65 Å. The use of the two reflections at this

 ©2001 The American Physical Society

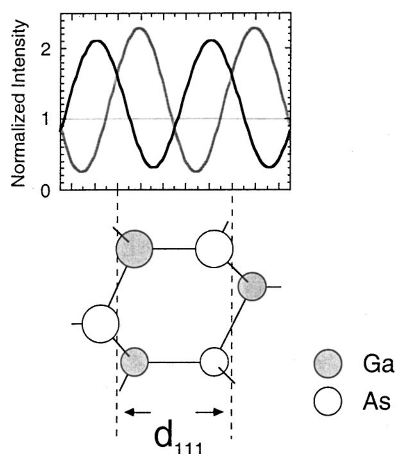

FIG. 1. Theoretical calculations of the normalized electric-field intensity for the GaAs(111) (shaded line) and GaAs($\bar{1}\bar{1}\bar{1}$) (bold line) Bragg back-reflections conditions at photon energy $\hbar\omega = 1900.05$ eV. This photon energy maximizes the electric-field intensity on the Ga atomic planes for the (111) reflection and on the As atomic planes for the ($\bar{1}\bar{1}\bar{1}$) reflection. The spatial positions of the electric-field intensities within the crystalline-unit cell are shown relative to the Ga and As atomic planes. The dotted line represents the normalized electric-field intensity away from the Bragg condition, which is constant and equal to 1.

particular photon energy maximizes the contrast between the emission from the Ga and As atoms, as determined by a previous scanned x-ray standing-wave experiment.[12] The field intensities in Fig. 1 have been normalized to the electric-field intensity away from the Bragg condition where $R=0$. At photon energy $\hbar\omega=1900.05$ eV, the phase difference ν between the incident and reflected fields is such that the maximum of the electric-field intensity is close to the Ga atomic planes for the GaAs(111) reflection, and close to the As atomic planes for the GaAs($\bar{1}\bar{1}\bar{1}$) reflection. Significant contrast between the Ga and As contributions to both the core and valence electron-emission spectra can therefore be obtained for this heteropolar zinc-blende crystal under these experimental conditions.

The experiment was performed at the Stanford Synchrotron Radiation Laboratory using the ''Jumbo'' double-crystal monochromator and a standard, ultrahigh-vacuum chamber. Figure 2 shows the Ga and As core and valence electron-emission spectra in the vicinities of the GaAs(111) and GaAs($\bar{1}\bar{1}\bar{1}$) Bragg back-reflection conditions. The spectra were recorded with a double-pass cylindrical mirror analyzer operating with x-ray photoelectron slits at a pass energy of 50 eV to give an electron-energy resolution of $\sim$0.8 eV. The monochromator was operated with a pair of InSb(111) crystals to give a photon-energy width of $\sim$0.7 eV. The photon energy used to record each spectrum ($\hbar\omega=1900.05$ eV) places the maximum of the electric-field intensity on either the Ga or As atomic planes for the GaAs(111) and the GaAs($\bar{1}\bar{1}\bar{1}$) reflections, respectively, as described above, and as verified by photon-energy scanned x-ray standing-wave measurements of the Ga and As $3d$ core levels.

The data exhibit the well-known x-ray standing wave effect[13] for both the Ga $3d$ and the As $3d$ core levels, as well as for the crystal valence band. We note that the emission

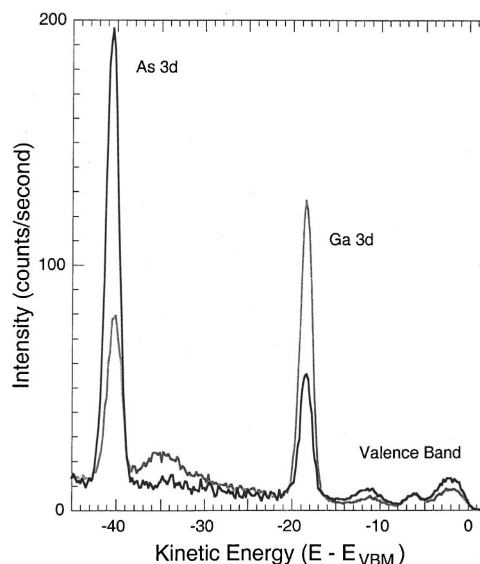

FIG. 2. Comparison of the photoemission spectra, referenced to the valence-band maximum, for the GaAs(111) (shaded lines) and GaAs($\bar{1}\bar{1}\bar{1}$) (bold lines) reflections over the kinetic-energy range of the Ga $3d$, As $3d$, and valence-electron emission. For the GaAs(111) reflection, the maximum of the electric-field intensity was placed close to the Ga atomic planes. For the GaAs($\bar{1}\bar{1}\bar{1}$) reflection, the maximum of the electric-field intensity was placed close to the As atomic planes. Note the enhancement of the emission from the on-atom atomic planes and the suppression of the emission from the off-atom atomic planes in each case.

from either of the preferentially excited Ga or As atomic planes is enhanced by over a factor of 2 relative to its emission from the alternate condition where it is suppressed. In a standard x-ray standing-wave experiment, the maximum of the electric-field intensity is scanned through the crystalline-unit cell by experimentally varying the phase ν of the complex reflectivity function, while the intensity of a core, Auger, or fluorescence line is monitored to locate the position of a particular atom within the unit cell. Our experiment is a departure from the standard x-ray standing-wave technique in that we selectively position the maximum of the electric-field intensity within the crystalline-unit cell, and then record high-resolution valence photoelectron spectra in a fixed electric-field condition to produce spatially resolved valence electronic structure.

Figure 3 compares the valence-band regions of the spectra from Fig. 2. Note the large differences between the two electronic structures, dependent on which of the atomic planes; i.e., either the anion or cation atomic planes, was preferentially excited. The features at the lowest and highest kinetic energies are enhanced when the maximum of the electric-field intensity is placed on the As electronic cores, whereas the feature at intermediate kinetic energy is enhanced when the maximum of the electric-field intensity is placed on the Ga electronic cores.

From the theoretical calculations of Cohen and Chelikowsky,[14] it is well established that the three lobes observed in the valence band of GaAs, which are typical of covalent semiconductors,[14,15] are directly correlated with the crystalline band structure; they arise from the hybridization of the Ga and As $4s$ and $4p$ orbitals. The first lobe corre-

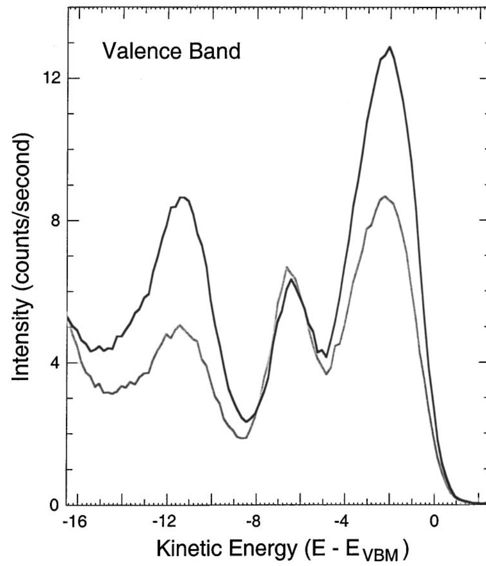

FIG. 3. Comparison of the Ga (shaded line) and As (bold line) GaAs valence-photoemission spectra from Fig. 2. Note the sensitivity of the spectra to the location of the electric-field intensity within the crystalline-unit cell. The features at the lowest and highest binding energies are enhanced when the maximum of the electric-field intensity is placed on the As atomic cores, whereas the feature at intermediate kinetic energy is enhanced when the maximum of the electric-field intensity is placed on the Ga atomic cores.

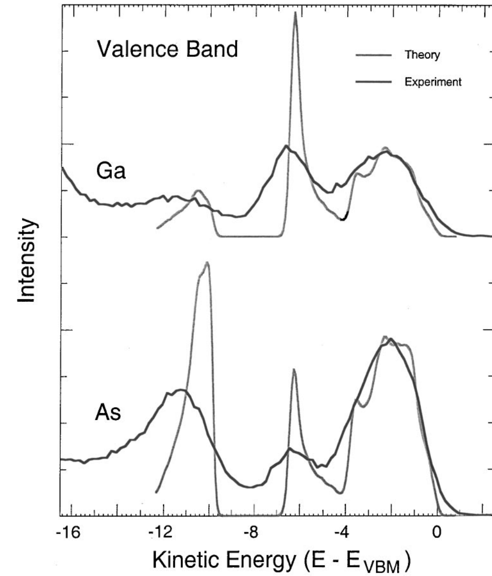

FIG. 4. Comparison of the *chemically resolved* Ga and As contributions to the GaAs valence band with the theoretically calculated Ga and As partial density of states. The upper portion of the figure shows the cation contributions, and the lower portion of the figure shows the anion contributions. The spectra have been offset for clarity.

sponds to the most tightly bound-electron band; the electronic states within this lobe are strongly localized on the As-anion sites and originate from the As atomic $4s$ level. The second lobe is more complex, and the character of the electronic states changes from Ga-cation $4s$ to As-anion $4p$ with increasing kinetic energy going from the band edge to the band maximum. The third lobe includes the top two valence bands; it extends to the valence-band maximum and is mostly of As-anion $4p$ character. Clearly, these theoretical conclusions are immediately evident even in our raw data.

In order to uniquely resolve the individual Ga and As contributions to the GaAs valence band, we proceed as follows. Under the condition of constant electric-field intensity, the valence photocurrent can be approximated as the linear sum of the individual partial-density of states $\rho_i(E)$ arising from the different i atoms of the crystalline-unit cell weighted by the energy-dependent, relative cross sections $\sigma_i(E,\hbar\omega)$ of each of the states:[4,6,16]

$$I(E,\hbar\omega)\propto\Sigma_i\rho_i(E)\sigma_i(E,\hbar\omega). \quad (3)$$

For the case of a spatially dependent x-ray field, it is easily shown that this expression must be modified to include the electric-field intensities at each of the different atomic-core positions:[17]

$$I(E,\hbar\omega)\propto\Sigma_i\rho_i(E)\sigma_i(E,\hbar\omega)[1+R+2\sqrt{R}\cos(\nu+\mathbf{h}\cdot\mathbf{r}_i)]. \quad (4)$$

Note that when $R=0$, i.e., away from the Bragg condition, the above expression reduces to Eq. (3). Equation (4) contains the individual contributions to the valence-electron spectrum $\rho_i\sigma_i$ multiplied by the electric-field intensities at the position of each of the atomic sites. Hence for a two atom unit cell such as GaAs, all that is necessary to uniquely resolve the individual chemical components of the GaAs valence band is to obtain valence spectra at two different electric-field conditions and then solve a simple set of two linear equations. The coefficients of the individual components to the valence spectra are the relative electric-field intensities at the Ga and As atomic sites; they may either be calculated theoretically, as in Fig. 1, or determined experimentally from the core-level data shown in Fig. 2.

Figure 4 shows the resulting *chemically* resolved components of the GaAs valence band obtained by taking the appropriate linear combinations of the spectra from Fig. 3. These components are compared to an *ab initio* theoretical calculation of the Ga and As partial-density of states. Indeed, the difference between the Ga- and As-related curves is greatly enhanced with respect to Fig. 3. The calculations were performed by using *ab initio* pseudopotentials within density-functional theory, with a plane-wave basis.[14] We used Troullier-Martins pseudopotentials[18] cast into the separable Kleinman-Bylander form[19] and the local-density exchange-correlation functional of Ceperely and Adler.[20] The experimental GaAs lattice parameter of 5.65 Å was used. A cutoff energy greater than 20 Ryd and a k-point sampling greater than 150 points in the irreducible Brillouin zone were used to guarantee convergence. Site-specific density of states curves were computed by using a sphere of 1.22 Å radius (corresponding to the covalent radius), centered on each atom, to deconvolve the obtained wave functions over atomic orbitals of valence electrons. The resulting density of states was only very weakly dependent on the radius chosen, within a range of several tenths of angstroms around this radius.

The calculations clearly show the differences between the two electronic structures centered around each atomic core.

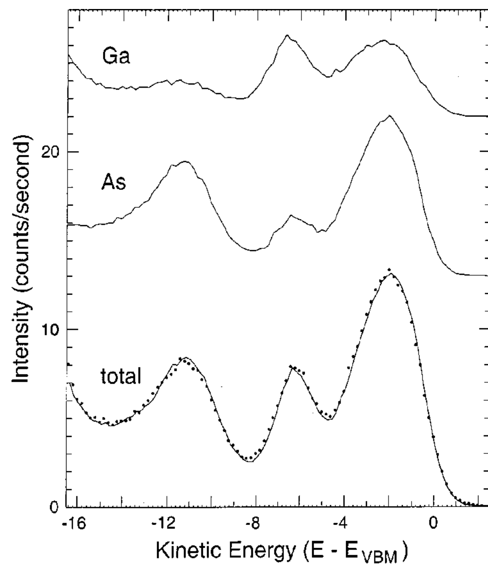

FIG. 5. Chemically resolved Ga and As contributions to the GaAs valence band. The top curve shows the cation emission, and the middle curve shows the anion emission. The bottom curves compare a valence spectrum recorded off the Bragg condition (dots) with the sum of the individual anion and cation components (solid line). The spectra have been offset for clarity.

These differences occur due to the natural ordering of the atomic Ga and As $4s$ and $4p$ valence states, coupled with the solid-state bonding that has occurred between them. Remarkable qualitative agreement between the theory and experiment is observed. Note that the calculations do not take into account either the experimental resolution or the relative photoionization cross sections of Eqs. (3) and (4); however, for the given choice of atomic radii, the similarity between the theoretical and experimental spectra suggests that atomic cross-section effects are unimportant for the understanding of the gross spectral features.

In order to further evidence the general validity of our approach, Fig. 5 compares a valence spectrum recorded off the Bragg condition (dots) with the sum of the individual Ga and As components (solid line). Away from the Bragg condition, the electric-field intensity is constant over the dimensions of the crystalline-unit cell, so the valence spectrum should appear as the simple linear sum of the anion and cation contributions [Eq. (3)]. Note that the two spectra are indistinguishable within the experimental uncertainties, thereby experimentally validating the linear decomposition of the photoemission density of states according to Eqs. (3) and (4).

In conclusion, we have demonstrated that valence-photoelectron spectra recorded in the vicinity of a crystal x-ray Bragg reflection can reveal site-specific valence information that is directly related to the partial-density of occupied valence states. It is our hope that this method will provide useful information pertaining to the detailed electronic structure of more complex crystalline materials that are currently of interest to the scientific community.

E.J.N. thanks the National Research Council for support. This work was performed at the Stanford Synchrotron Radiation Laboratory which is supported by the United States Department of Energy, Office of Basic Energy Sciences. M.J., L.K., and J.R.C. would like to acknowledge support from the U.S. Department of Energy, the NSF and the Minnesota Supercomputing Institute.

[1] A. Einstein, Ann. Phys. (Leipzig) **17**, 132 (1905); **20**, 199 (1906).

[2] See, for example, *Photoemission in Solids I*, edited by M. Cardona and L. Ley, Topics in Applied Physics Vol. 26 (Springer-Verlag, Berlin, 1978); *Photoemission in Solids II*, edited by M. Cardona and L. Ley, Topics in Applied Physics Vol. 27 (Springer-Verlag, Berlin, 1978); *Photoelectron Spectroscopy: Principles and Applications*, 2nd ed., edited by S. Hufner (Springer-Verlag, Berlin, 1996).

[3] J. W. Cooper, Phys. Rev. **128**, 681 (1962).

[4] W. Braun *et al.*, Phys. Rev. B **10**, 5069 (1974).

[5] D. E. Eastman and J. L. Freeouf, Phys. Rev. Lett. **34**, 395 (1975).

[6] T.-U. Nahm, M. Han, S.-J. Oh, J.-H. Park, J. W. Allen, and S.-M. Chung, Phys. Rev. Lett. **70**, 3663 (1993); Phys. Rev. B **51**, 8140 (1995); T.-U. Nahm, R. Jung, J.-Y. Kim, W.-G. Park, S.-J. Oh, J.-H. Park, J. W. Allen, S.-M. Chung, Y. S. Lee, and C. N. Whang, *ibid.* **58**, 9817 (1998).

[7] U. Fano, Phys. Rev. **124**, 1866 (1961).

[8] L. Ley, M. Taniguchi, J. Ghijsen, R. L. Johnson, and A. Fujimori, Phys. Rev. B **35**, 2839 (1987); D. Brown, M. D. Crapper, K. H. Bedwell, M. T. Butterfield, S. J. Guilfoyle, A. E. R. Malins, and M. Petty, *ibid.* **57**, 1563 (1998); J. Okabayashi, A. Kimura, T. Mizokawa, A. Fujimori, T. Hayashi, and M. Tanaka, *ibid.* **59**, 2486 (1999).

[9] A. Stuck *et al.*, Phys. Rev. Lett. **65**, 3029 (1990).

[10] B. W. Batterman and H. Cole, Rev. Mod. Phys. **36**, 681 (1964).

[11] L. I. Schiff, *Quantum Mechanics* (McGraw-Hill, New York, 1968), Chap. 11.

[12] J. C. Woicik *et al.*, Phys. Rev. Lett. **84**, 773 (2000).

[13] D. P. Woodruff, D. L. Seymour, C. F. McConville, C. E. Riley, M. D. Crapper, N. P. Prince, and R. G. Jones, Surf. Sci. **195**, 237 (1988); J. Zegenhagen, Surf. Sci. Rep. **18**, 199 (1993).

[14] M. L. Cohen and J. R. Chelikowsky, *Electronic Structure and Optical Properties of Semiconductors*, Springer Series in Solid-State Sciences Vol. 75 (Springer-Verlag, Berlin, 1988), Chap. 6.

[15] L. Ley, R. A. Pollak, F. R. McFeely, S. P. Kowalczyk, and D. A. Shirley, Phys. Rev. B **9**, 600 (1974).

[16] In general, this sum should include the individual angular-momentum components of the density of states (Ref. 6); however, for simplicity we have written $\rho_i(E)\sigma_i(E,\hbar\omega) = \Sigma_j \rho_{i,j}(E)\sigma_{i,j}(E,\hbar\omega)$, where j is the angular momentum.

[17] J. C. Woicik *et al.* (unpublished).

[18] N. Troullier and J. L. Martins, Phys. Rev. B **43**, 1993 (1991).

[19] L. Kleinman and D. M. Bylander, Phys. Rev. Lett. **48**, 1425 (1982).

[20] D. M. Ceperley and B. J. Alder, Phys. Rev. Lett. **45**, 566 (1980).